Advances in Discontinuous Numerical Methods and Applications in Geomechanics and Geoengineering

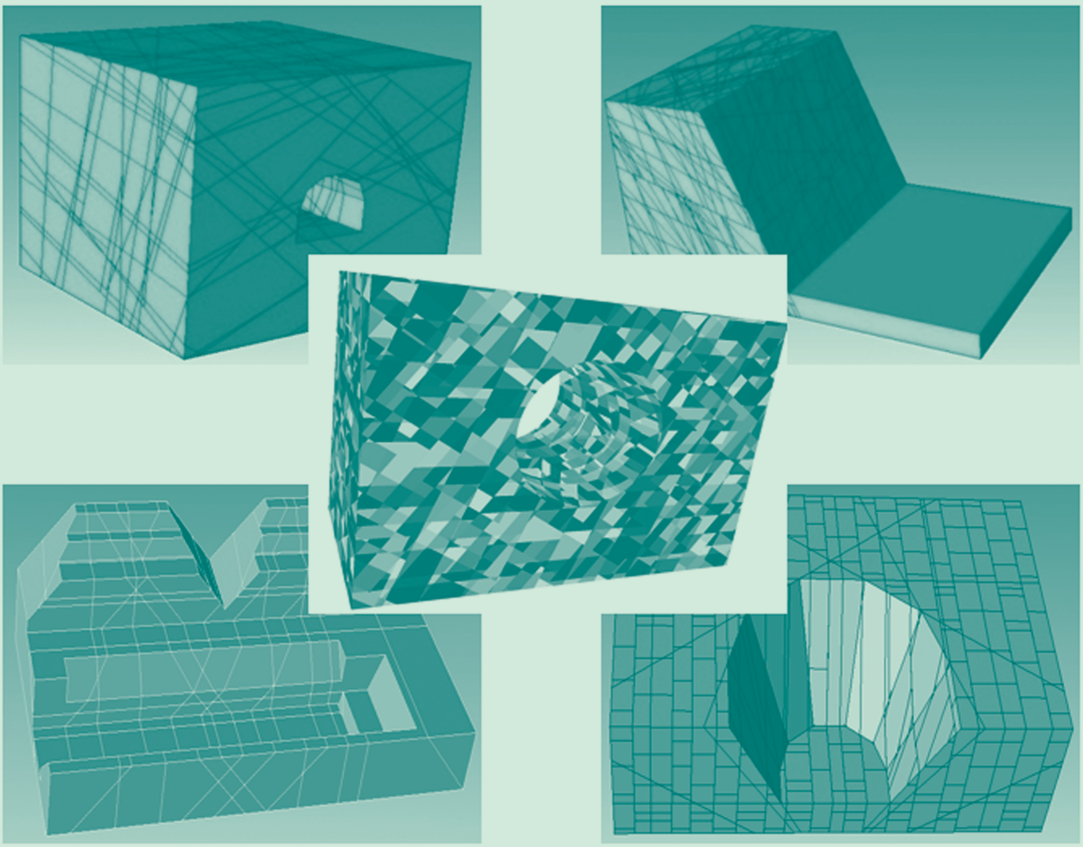

JIAN ZHAO
YUZO OHNISHI
GAO-FENG ZHAO
TAKESHI SASAKI
EDITORS

CRC Press
Taylor & Francis Group
A BALKEMA BOOK

ADVANCES IN DISCONTINUOUS NUMERICAL METHODS AND APPLICATIONS IN GEOMECHANICS AND GEOENGINEERING

This page intentionally left blank

PROCEEDINGS OF THE 10TH INTERNATIONAL CONFERENCE ON ADVANCES IN DISCONTINUOUS NUMERICAL METHODS AND APPLICATIONS IN GEOMECHANICS AND GEOENGINEERING, ICADD 10, HONOLULU, HAWAII, 6–8 DECEMBER 2011

Advances in Discontinuous Numerical Methods and Applications in Geomechanics and Geoengineering

Editors

Jian Zhao

Laboratory for Rock Mechanics
Ecole Polytechnique Fédérale de Lausanne
Lausanne, Switzerland

Yuzo Ohnishi

Kyoto University, Kyoto, Japan

Gao-Feng Zhao

School of Civil and Environmental Engineering
The University of New South Wales, Sydney, Australia

Takeshi Sasaki

Rock Engineering Lab., Suncoh Consultants Co. Ltd., Tokyo, Japan

CRC Press
Taylor & Francis Group
Boca Raton London New York Leiden

CRC Press is an imprint of the
Taylor & Francis Group, an **informa** business
A BALKEMA BOOK

CRC Press
Taylor & Francis Group
6000 Broken Sound Parkway NW, Suite 300
Boca Raton, FL 33487-2742

Version Date: 20120201

International Standard Book Number-13: 978-0-203-11442-1 (eBook - PDF)

Visit the Taylor & Francis Web site at
http://www.taylorandfrancis.com

and the CRC Press Web site at
http://www.crcpress.com

This proceedings is a tribute to Dr Gen-Hua Shi for his innovatory works on Key Block Theory, Discontinuos Deformation Analysis and Numerical Manifold Method.

This page intentionally left blank

Advances in Discontinuous Numerical Methods and Applications in Geomechanics and Geoengineering – Zhao et al. (eds)
© 2012 Taylor & Francis Group, London, ISBN 978-0-415-68404-0

Table of contents

Advances in Discontinuous Numerical Methods and Applications in Geomechanics and Geoengineering – Zhao et al. (eds)
© 2012 Taylor & Francis Group, London, ISBN 978-0-415-68404-0

Preface

The proceedings of ICADD-10 is a collection of 56 technical papers, including 8 keynotes, accepted by the conference. ICADD-10 is the 10th event of the series since 1995. The conference series have been organised every 2–3 years focusing initially on the discontinuous deformation analysis method and gradually covering the discontinuous numerical methods and coupling techniques with other numerical approaches, for geomechanics and geoengineering.

Geomechanics can be viewed often as discontinuum mechanics, as rocks and soils can behave as discontinuous materials, physically and mechanically. Deformation and failure of rocks and soils often involve grain separation and interface movement. The discontinuous nature is inevitable in rock masses and granular soils. It was therefore, not surprised that the starting of the main discontinuous numerical methods, the distinct element method by Dr Peter Cundall in 1972, and discontinuous deformation analysis by Dr Gen-Hua Shi in 1985, all associated with rock mechanics.

Discontinuous numerical methods have now been widely applied in geoengineering related to civil, mining, hydropower and petroleum engineering. There are many good examples of using UDEC/3DEC and DDA in design and forensic of geoengineering projects, in dams, slopes, tunnels, caverns and mines. The discontinuous numerical methods provide good tools to capture the true physical and mechanical behaviours of the geomaterials, and provide the scientific insights enabling for better engineering design, by numerical modelling. Discontinuous numerical methods are indeed very much engineering tools of the present, and certainly more in the future.

As ICADD-10 marks the 10th event of the ICADD series, the conference focuses on review and progress, with the conference title "back to the Future". The papers included in this proceedings cover a wide scope of discontinuous numerical methods from algorithms and mechanics, to modelling techniques and applications, including the key block theory, the discontinuous deformation analysis, the numerical manifold method, the distinct/discrete element method, coupled discontinuum and continuum methods, multi-scale and multi-physics in modelling, applications and case studies of engineering projects.

ICADD-10 is jointly organised by the rock mechanics groups at the Ecole Polytechnique Fédérale de Lausanne (EPFL) in Switzerland and the University of Kyoto in Japan, and supported by the American Rock Mechanics Association (ARMA) and the Society for Rock Mechanics and Engineering Geology of Singapore (SRMEG). The conference organising committee is co-chaired by Jian Zhao and Yuzo Ohnishi, and teamed with Yuyong Jiao, Guowei Ma, Takeshi Sasaki, Liang Sun, Gao-Feng Zhao, and Yingxin Zhou. The publication of this proceedings is supported by Leon Bijnsdorp and Richard Gundel of CRC Press.

Jian Zhao, Yuzo Ohnishi,
Gao-Feng Zhao & Takeshi Sasaki
December 2011

This page intentionally left blank

Keynotes

This page intentionally left blank

Advances in Discontinuous Numerical Methods and Applications in Geomechanics and Geoengineering – Zhao et al. (eds)
 ISBN 978-0-415-68404-0

Rock block stability analysis of slopes and underground power houses

G.H. Shi
DDA Company, Terrace Drive, California, US

ABSTRACT: In the field of practical rock engineering, there are two independent computations: continuous computation and limit equilibrium computation. Limit equilibrium is still the fundamental method for global stability analysis. For any numerical method in rock engineering, reaching limit equilibrium requires large displacements, discontinuous contacts, precise friction law, multi-step computation and stabilized time-step dynamic computation. Therefore three convergences are unavoidable: convergence of equilibrium equations, convergence of open-close iterations for contacts and convergence of the contact forces of dynamic computations. This paper will cover key block theory, two dimensional Discontinuous Deformation Analysis (DDA), three dimensional joint cutting and a simple version of three dimensional DDA.

1 INTRODUCTION

The fundamental axiom of key block theory (Shi et al., 1985; Shi and Goodman, 1989) is that an excavation is completely safe only if the key blocks are adequately supported. A key block is a complete convex or concave block (or their unions) having a face on the understructure surface, and the other faces formed by pre-existing joint planes. The key block theory can be applied to the design of the support and the lining of tunnels in jointed hard rocks. For jointed rock masses, block theory has distinct advantages over stress/strain formulations; it makes full use of the joint sets, friction angles and the statistical data of joint spacing and lengths, and relates directly to the real joint map; the support placement and design detail can be accurately estimated; and the correctness of the designs can be verified directly and adjusted to practical experience during a project. However, when the in situ stress is very high or the rock strength is low, new joints or failure surfaces may be produced, accompanying slabbing, shearing or bending failure of the rock. Blocky theory is incapable of predicting these types of failure and should not be used alone for such situations.

The original purpose of Discontinuous Deformation Analysis (DDA) (Shi and Goodman, 1985; Shi, 1988) was to solve inverse problems, e.g., to compute the Young's modulus and the Poisson's ratio from displacement measurements. The DDA backward analysis can perform an accurate interpretation of measured displacements and offers material constants, initial stresses of the rock mass or possible boundary conditions for further analysis. The forward DDA analysis can predict future states of stabilities for the jointed rock masses. The combination of the forward and backward DDA is a complete practical numerical analysis procedure for problems in jointed rock masses. The DDA provides a unique solution for large displacement and failure computations of block structures for rock engineering. It can analyze the mechanical response of rock block systems under general loading and boundary conditions with rigid body movement and deformation occurring simultaneously. Large displacements and deformations are considered under both static and dynamic loadings. Because sliding and opening of block contacts are the dominant factors in failure, the DDA can determine damage and failure mechanisms for block systems. Applications of DDA were pursued in various areas of rock and mining engineering (Shi, 1999). Compared with key block theory, the disadvantages of DDA are: (i) the computational requirement is more demanding; (ii) the 3-D implementation is complex.

For global stability analysis, the block sliding is a main issue. The computation must use a process of cutting blocks from statistically generated joint polygons and measured polygons in 3D space (Shi, 1993; Shi, 2002). The rock mass connectivity depends on the joint length ratio. The joint length ratio is joint length divided by joint spacing. If the joint length ratio is less than 10, the rock masses are likely connected; if this joint length ratio is greater than 10, the rock is likely to be blocky. In all the cases of this paper the rock masses are considered to be blocky or discontinuous. The algorithm must work for both joint sets and for any joint system where each joint has its own direction. Based on the produced joint blocks, the algorithm of finding removable blocks is used for the computation.

In this paper, applications of key block theory on estimation of the removable blocks of a underground power house, 2D-DDA on stability analysis of transportation tunnel and slopes, 3D joint cutting method on estimation of removable blocks of surge chamber system and 3D-DDA on stability analysis of slope will be presented.

2 REMOVABLE BLOCK ESTIMATION USING KEY BLOCK THEORY

2.1 *Geological and geometric data of the rock mass*

Table 1 below gives the joint set orientations of the surrounding rock masses that the key block analysis are performed for the stability of the underground power house.

2.2 *Key block computation of all possible combination of key blocks*

Giving the orientation (dip angle and dip direction angle) of each joint set, the whole space stereographic projection can be drawing which is the diagram of all the removable joint pyramids. Giving the orientation (strike and dip) of the axis and the section shape of the underground power house, the maximum removable block area of each joint pyramid is drawn together with the joint pyramid code and the mode of sliding.

Figures 1 and 2 are whole space stereographic projection drawing for finding removable blocks of tunnels. The projection of each joint set is a solid circle. The projection of a free plane is a dashed circle. Each area intersected by the solid circles is the projection of a joint pyramid JP. In Figure 1, the JP codes are printed in the corresponding area. For example, 110 has the following meaning: (i) the first digit "1" means lower side of joint set 1; (ii) the second digit "1" means lower side of joint set 2; and (iii) the third digit "0" mean upper side of joint set 3.

In Figure 1, the maximum removable block area of each joint pyramid is drawn together with the joint pyramid code and the sliding force of unit weight. In Figure 2, the maximum removable block area of each joint pyramid is drawn together with the mode of sliding and the factor of safety. Mode of sliding is the sliding joint planes: (i) "3" means the block slides along the joint plane 3 only; (ii)"12" means the block slides along the intersection line of joint planes 1 and 2.

The friction angle of joint sets 1, 2 and 3 are 20.0. Under these friction angles and 0 cohesions, Figure 1 shows the sliding force of unit weight in the second row in each JP area. Figure 2 shows the factor of safety in the second row in each JP area. From Figure 1, the

Table 1. Joint set orientations.

Joint set	Dip angle	Dip direction
1	35°	315°
2	70°	150°
3	85°	25°

Figure 1. Finding removable block code and maximum key block area with sliding forces by whole stereographic projection.

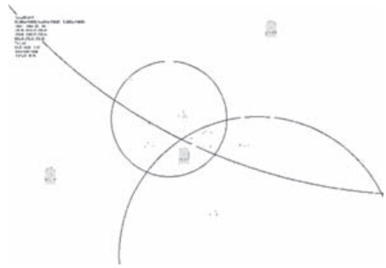

Figure 2. Finding sliding modes and maximum key block area with factor of safety by whole stereographic projection.

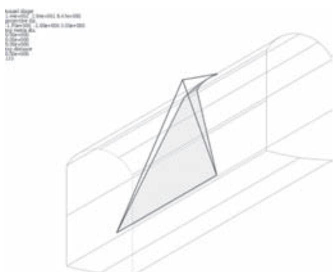

Figure 3. Maximum key block JP = 110 of the underground power house.

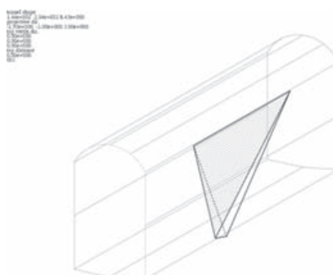

Figure 4. Maximum key block JP = 001 of the underground power house.

sliding force of unit weight of the removable block JP = 111 is 1.00. This is direct falling mode. From Figure 2, the factor of safety of removable block JP = 110 is 0.03 without support and under the given friction angle. The first row of this area is “3”. It means the block slide along joint set 3.

2.3 *Maximum key blocks of each combination*

For each joint pyramid with removable block area, the maximum removable block is drawn. The maximum removable block is not a real key block, which is computed under assumption that the joints in each joint set are infinitely long and infinitely dense.

The real removable blocks is generally much smaller and with the same shape comparing with the maximum removable block with the same joint pyramid code. Figure 3, Figure 4 are the maximum key block drawing of JP code 110 and 001. The real key block of the same JP code is much smaller with the joint planes parallel to the joint planes of corresponding maximum key block.

2.4 *Finding key block interval on tunnel boundary by whole space stereographic projection*

The joint data of Table 2 are the orientation, the average length and average spacing of the four joint sets used for the underground power house stability analysis using the key block theory. Similar to the previous section, the joint pyramid (JP) with removable blocks are identified. These JP codes will be the input data of the unroll program.

2.5 *Unroll maps of joint traces and key blocks*

Based upon the orientation of the joint sets, the axis direction, the section shape, the average length and the average spacing of joints in each joint set of the underground power house, the

Table 2. Joint set angle data.

Joint set	Dip angle	Dip direction	Spacing S_{3d}	Length L_{tr}	Bridge
1	35°	315°	3.00 m	45.0 m	0.2 m
2	70°	150°	55.0 m	1000.0 m	3.0 m
3	85°	25°	2.00 m	10.0 m	3.0 m
4	85°	58°	2.00 m	10.0 m	4.0 m

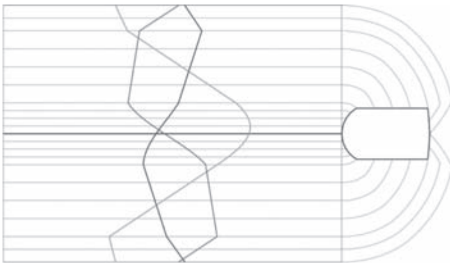

Figure 5. The general unroll curve of all four joint sets.

Figure 6. The unroll map of statistically produced joint traces of all four joint sets on the surface of the underground power house.

Figure 7. The projection map of statistically produced joint traces of all four joint sets on the surface of the underground power house.

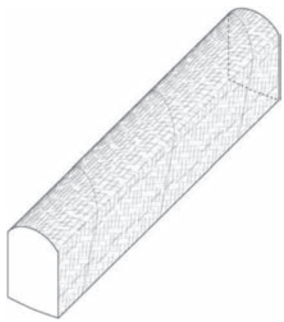

Figure 8. The projection map of statistically produced joint traces of all four joint sets on the surface of the underground power house with the opposite projection direction.

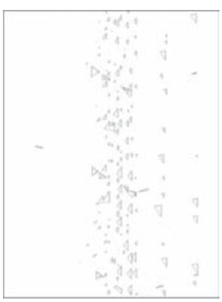

Figure 9. The removable blocks on the unroll map of statistically produced joint traces of all four joint sets on the surface of the underground power house.

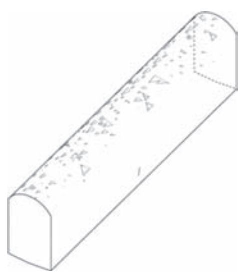

Figure 10. The projection drawing of removable blocks on statistically produced joint trace map of all four joint sets on the surface of the underground power house.

joint unroll map is produced. Using the produced joint trace map, the removable blocks are delimited for each joint pyramid with removable blocks. It can be seen there are no major key blocks. All of the removable block can be well supported by the distributed bolts.

Figure 5 shows the general unroll curve of all four joint sets. Figure 6 shows the unroll map of statistically produced joint traces of all four joint sets on the surface of the underground powerhouse. Figure 7 and Figure 8 are the projection maps of the same statistically produced joint traces of all four joint sets on the surface of the underground power house viewing from two opposite projection directions. Figure 9 shows the removable blocks on the unroll map of the same statistically produced joint traces of all four joint sets on the surface of the underground powerhouse. All of the removable blocks are in small size. The distributed systematic bolts can fix these small size removable blocks. Figure 10 shows the projection drawing of removable blocks on statistically produced joint trace map on the surface of the underground powerhouse. Two opposite projection directions are used. It also can be see, all of the removable blocks are in small size.

3 BLOCK STABILITY ANALYSIS OF TRANSPORTATION TUNNELS USING 2D DDA

Transportation tunnels have variable directions and curved axes. Block stability analysis are carried out using 2D-DDA. Under the same joint sets and joint set geometry, 5 tunnel sections of difference axis directions are computed, starting from N36E rotating clockwise 35 degrees for each new section. The computation result shows the rock falling of the different tunnel sections is different. After bolting, this whole tunnel is safe with considerable safety margin.

3.1 *General geological condition of transportation tunnels*

Table 3 gives the joint set directions and geometry and Table 4 gives the physical data of the rock masses for all the 5 tunnel sections.

3.2 *Rock falling and bolt reinforcements of section 1*

Figures 11 and 12 show the 2D-DDA computation result of the tunnel section 1 (N36E) with bolts. It can be seen 6 small key blocks in between the bolts will fall. The spacing of the bolts along the tunnel axis is 1 meter. The falling process and final pattern of the transportation tunnel are shown in Figures 13 and 14.

Table 3. Joint set orientation, joint spacing and joint trace length.

Joint set	Dip angle	Dip direction	Spacing S_{3d}	Length L_{tr}	Bridge
1	40°	295°	0.75 m	30.0 m	0.10 m
2	70°	105°	0.45 m	7.00 m	3.00 m
3	65°	150°	1.50 m	10.0 m	7.50 m

Table 4. Physical data of tunnel rock mass.

Unit weight ton/cubic meter	2.7
Elastic modulus ton/square meter	3000000
Poisson's ratio	0.25
Friction angle degree	25
Cohesion ton/square meter	0

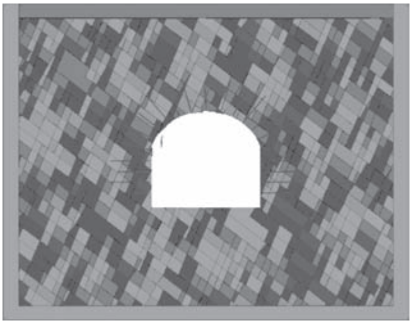

Figure 11. Bolting computation of transportation tunnel of axis N36E.

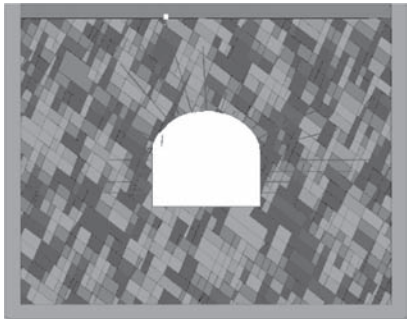

Figure 12. Bolting forces of transportation tunnel of axis N36E.

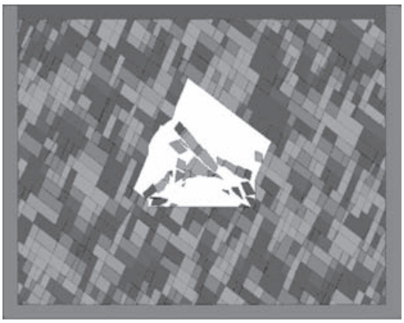

Figure 13. Rock falling process of transportation tunnel of axis N36E.

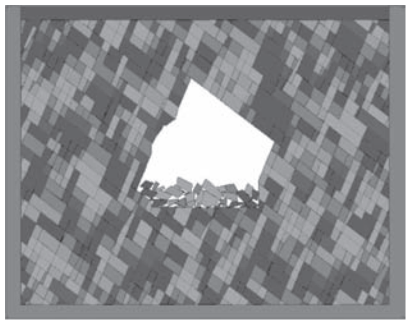

Figure 14. Rock falling result of transportation tunnel of axis N36E.

4 TWO DIMENSIONAL DDA STABILITY COMPUTATION OF SLOPES

4.1 *2D-DDA stability and bolting computation of slope section 1*

The slope section 1-1 of the dam abutment is computed here. As the cohesion is too sensitive in the sliding stability computation, zero cohesion is assumed here. For section 1-1, the computation shows the maximum cable tension force is 99 ton. The average tension force of the cables which are on the relatively small key block is less than 99 Ton. Here the friction angle is 18 degrees and the cohesion is zero. The stable friction angle is 25 degrees without cable and cohesion. Table 5 is the physical data of the rock mass used by 2D-DDA computation for all sections 1-1 to 9-9.

2D-DDA only computes a section of the rock without constrain of the side rock masses. The actual 3D fall should be much fewer in general. Therefore generally speaking, 2D-DDA results are conservative and can be accepted by the engineers. Figure 15 shows the 2D-DDA computation result of the section 1-1 on the dam abutment by using 25 degrees friction angle and 0 cohesion where the results shows the stable condition. Figures 16 and 17 show the rock sliding process of the section 1-1 on the dam abutment without cables. The friction angle is 20 degrees. The cohesion is 0. The computation has been done by 2D-DDA. Figure 18 shows the 2D-DDA computation result of the slope section 1-1 with cables. It can be seen no key blocks slide. The spacing of the cables is 4 meter. Figure 19 shows the resulting tension forces of all cables. The friction angle is 18 degrees. The cohesion is 0. The lengths of the purple color lines are proportional with tension force of the corresponding cables. Here for this section, maximum tension force is 99 tons. Similar analyses are carried out for other sections, e.g., Figure 20.

Table 5. Physical data of rock mass.

Unit weight ton/cubic meter	2.7
Elastic modulus ton/square meter	3000000
Poisson's ratio	0.25
Friction angle degree	19–25
Cohesion ton/square meter	0

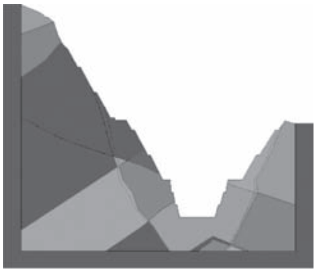

Figure 15. 2-d DDA computation result of the section 1-1 on the dam abutment by using 25 degree friction angle where the graphic output shows the stable condition.

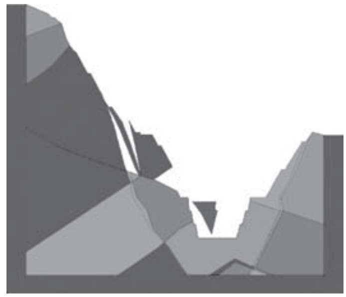

Figure 16. Failure process computed by 2-d DDA of the section 1-1 on the dam abutment by using 20 degree friction angle.

Figure 17. Failure condition computed by 2-d DDA of the section 1-1 on the dam abutment by using 20 degree friction angle.

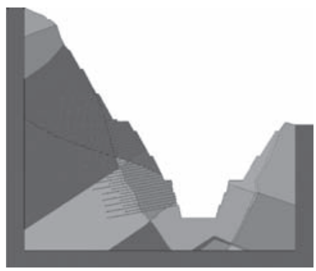

Figure 18. 2-d DDA bolting computation of the section 1-1 on the dam abutment by using 18 degree friction angle where the graphic output shows the stable condition.

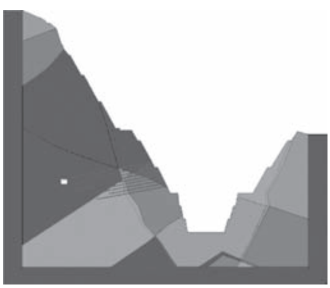

Figure 19. Resulting bolting forces giving by 2-d DDA bolting computation of the section 1-1 on the dam abutment by using 18 degree friction angle where the graphic output shows the stable condition.

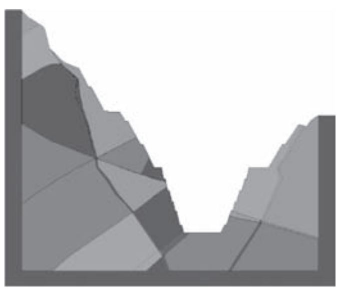

Figure 20. 2-d DDA computation result of the section 2-2 on the dam abutment by using 25 degree friction angle where the graphic output shows the stable condition.

5 REMOVABLE BLOCK ESTIMATION BY 3-D JOINT CUTTING METHOD

5.1 *Geological and geometry data of surge chamber joint sets*

In this section, the cutting program and other programs of 3D-DDA are used for finding key blocks of surge chamber tunnel system underneath underground power house. Joint polygons are produced based on the geometric data of joint sets. Based on produced joint polygons and input geometry of the surge chamber tunnel system, blocks are computed by the cutting program DC. The excavation program DA divided the excavated rock blocks from the unexcavated rock blocks. The key blocks are found by program DB based on block geometry, excavation surfaces and moving directions. The excavation surface here is the surface of the surge chamber tunnel system. Table 8 gives the input data for producing joint polygons of each joint set.

5.2 *Statistically produced joint polygons for each set of surge chamber rocks*

Figures 21, 22, 23 and 24 are the statistically produced joint polygons of joint set 1, 2, 3 and 4 respectively. The input data for producing joint polygons are joint set orientation data and joint set geometry data of Table 6.

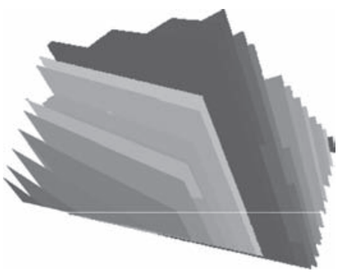

Figure 21. Statistically produced joint polygons of joint set 1.

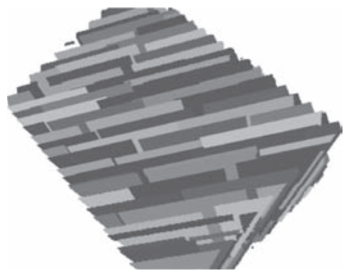

Figure 22. Statistically produced joint polygons of joint set 2.

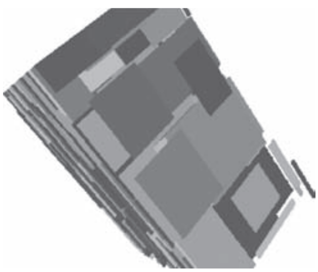

Figure 23. Statistically produced joint polygons of joint set 3.

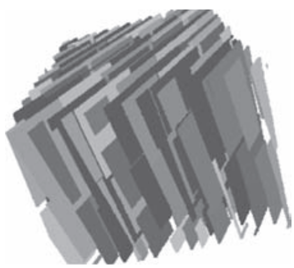

Figure 24. Statistically produced joint polygons of joint set 4.

Table 6. Joint set angle data.

Joint set	Dip angle	Dip direction	Spacing S_{3d}	Length L_{tr}	Bridge
1	35°	315°	5.00 m	500.0 m	4.00 m
2	70°	150°	4.00 m	40.0 m	1.00 m
3	85°	25°	5.00 m	30.0 m	1.00 m
4	85°	58°	5.00 m	30.0 m	1.00 m

Figures 25 and 26 are the same surface of the surge chamber tunnel system viewing from different directions. The shape of the surge chamber tunnel system is produced by parameters including the width, height, arch height and the shape code of each tunnel section.

5.3 *Rock blocks produced by surge chamber joint polygons*

Figure 27 shows one fifth of the blocks computed by program DC. The total number of blocks is 7739. The blocks are computed based on produced joint polygons and input geometry of the surge chamber tunnel system, blocks are computed by the cutting program DC.

5.4 *Delimited removable blocks from surge chamber rock blocks*

Figures 28, 29, 30 and 31 are the same group of maximum removable blocks. All these maximum removable blocks are found and colored by pink. The maximum removable blocks are searched under all possible sliding directions. All possible removable block are included in this group of maximum removable blocks. It can be seen from these figures, these pink color blocks are removable. Other word, there is a direction, the pink block can move directly into the surge chamber tunnel system and portals without moving other blocks.

5.5 *Delimited removable blocks from surge chamber produced by another statistically produced joint polygon systems*

Figures 31, 32, 33 and 34 are the same group of maximum removable blocks. The blocks are produced by other statistically produced joint polygons. All these maximum removable blocks are found and colored by pink. The sizes, shapes and even the distributions of the removable blocks are similar with the previous cases shown by Figures 27, 28, 29 and 30.

Figure 25. Surfaces of surge chamber tunnel system.

Figure 26. Surfaces of surge chamber tunnel system viewing from another direction.

Figure 27. One fifth of the produced blocks by joint cutting program where all statistically produced joint polygons and surge chamber tunnel system surface polygons are input.

Figure 28. Removable blocks of surge chamber tunnel system found by special searching program.

Figure 29. Removable blocks of surge chamber tunnel system found by special searching program and the excavated blocks.

Figure 30. Removable blocks of surge chamber tunnel system found by special searching program and the excavated blocks viewing from another direction.

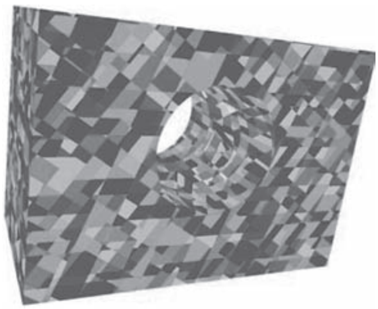

Figure 31. Removable blocks of surge chamber tunnel system found by special searching program and surrounding rock blocks.

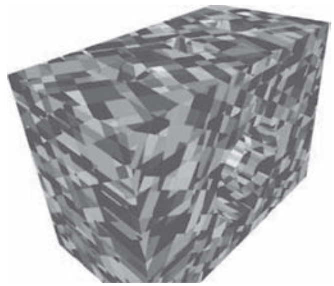

Figure 32. Removable blocks of surge chamber tunnel system found by special searching program and surrounding rock blocks using an alternative statistical data.

Figure 33. Removable blocks of surge chamber tunnel system found by special searching program and the excavated blocks using an alternative statistical data.

Figure 34. Removable blocks of surge chamber tunnel system found by special searching program using an alternative statistical data.

6 STABILITY ANALYSIS OF SLOPE USING KEY BLOCK THEORY AND 3D-DDA

6.1 *The stability estimation of the major block*

The major block is in the area of dam abutment. Assuming the slope surface is a plane, the volume of the major block is 1.13 million cubic meters. Due to its importance, different methods are used for its stability here: block theory, simple 3D-DDA and joint cutting method. The mode of the sliding is double face sliding which will offer relatively higher

Table 7. Joint set orientation.

Joint set	Dip angle	Dip direction
1	50°	180°
2	75°	115°
3	62°	70°

Table 8. Physical data of tunnel rock mass.

Unit weight ton/cubic meter	2.8
Elastic modulus ton/square meter	2000000
Poisson's ratio	0.25
Friction angle of joint 1: degree	17
Friction angle of joint 3: degree	26
Cohesion ton/square meter	0

factor of safety. Both block theory and 3D-DDA have basically the same result: considering the cohesion = 0 and the pre-tension of the cables the factor of safety is from 1.10 to 1.35 depend upon the assumption on the friction angles of two sliding faces.

6.2 *Geology and geometry data of the major block*

The geology data of the rock mass of this computation is listed in Tables 7 and 8.

6.3 *Finding removable blocks using whole space stereographic projection*

The computation loading of Figures 35 and 36 is under gravity without cable tension forces. Figures 35 and 36 are whole space stereographic projection drawing for finding removable blocks. The projection of each joint set is a solid circle. The projection of a free plane is a dashed circle. Each area intersected by the solid circles is the projection of a joint pyramid JP.

In Figure 35, the JP codes are printed in the corresponding area. For example, 001 has the following meaning: the first digit "0" means upper side of joint set 1, the second digit "0" means upper side of joint set 2 and the third digit "1" mean lower side of joint set 3. The yellow area with JP code 000 is entirely included inside the dashed circle. This means the block with JP code 000 is removable or key block. Again "000" represents: the first digit "0" means upper side of joint set 1, the second digit "0" means upper side of joint set 2 and the third digit "0" mean upper side of joint set 3.

From Figures 35 and 36, the friction angles of joint set 1, 2, and 3 are 19.7, 19.7 and 26 degrees respectively. Under these friction angles and 0.0 cohesions, Figure 35 shows the sliding force of unit weight in the second row in JP each area. Figure 36 shows the factor of safety in the second row in each JP area.

From Figure 35, the sliding force of unit weight of the removable block JP = 000 is 0.21. Sliding force is positive. Block is unstable. From Figure 36, the factor of safety of removable block JP = 000 is 0.67 without support and under the given friction angle. The first row of this area is "13". It means the block slide along the intersection of joint set 1 and joint set 3.

The computation loading of Figures 37 and 38 is under gravity. Cable tension forces are considered. Figures 37 and 38 are whole space stereographic projection drawing for finding removable blocks. The projection of each joint set is a solid circle. The projection of a free plane is a dashed circle. Each area intersected by the solid circles is the projection of a joint pyramid JP.

In Figures 37 and 38, the JP codes are printed in the corresponding area. The codes here represent the same meaning as those in the previous sections. From the figures, the friction

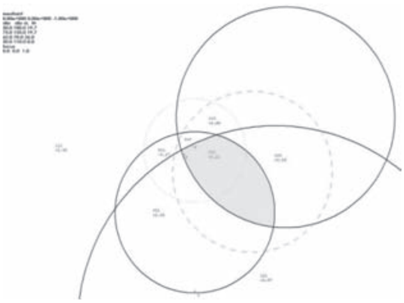

Figure 35. Finding key block and sliding force by whole stereographic projection.

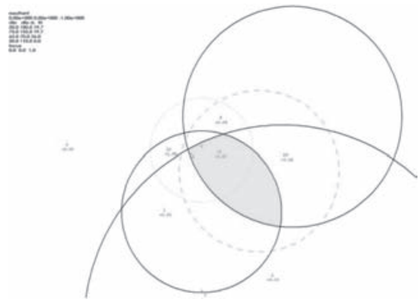

Figure 36. Finding sliding modes and factor of safety by whole stereographic projection.

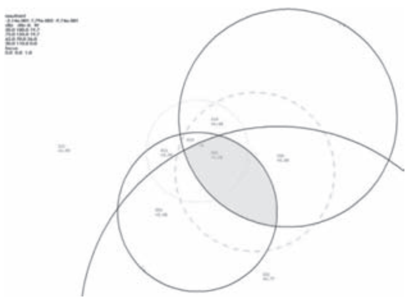

Figure 37. Finding key block and sliding force by whole stereographic projection.

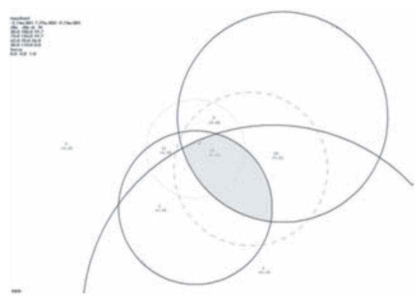

Figure 38. Finding sliding modes and factor of safety by whole stereographic projection.

angle of joint set 1, 2, and 3 are 19.7, 19.7 and 26 degrees respectively. Under these friction angles and 0.0 cohesions, Figure 37 shows the sliding force of unit weight in the second row in JP each area. Figure 38 shows the factor of safety in the second row in each JP area.

From Figure 37, the sliding force of unit weight of the removable block JP = 000 is –0.05. Sliding force is negative. Block is stable. From Figure 38, the factor of safety of removable block JP = 000 is 1.10 with support and under the given friction angle. The first row of this area is "13". It means the block slide along the intersection of joint set 1 and joint set 3.

The computation loading of Figure 39 is under gravity. Cable tension forces are considered. Figure 39 is whole space stereographic projection drawing for finding removable blocks. The projection of each joint set is a solid circle. The projection of a free plane is a dashed circle. Each area intersected by the solid circles is the projection of a joint pyramid JP. The yellow area with JP code 000 is entirely included inside the dashed circle. This means the block with JP code 000 is removable or key block.

Considering the first joint is not continuous, the friction angle of joint set 1, 2, and 3 are 25.9, 19.7 and 28 degrees respectively. Under these friction angles and 0.0 cohesions, Figure 39 shows the factor of safety in the second row in each JP area. From Figure 39, the factor of safety of removable block JP = 000 is 1.31 without support and under the given friction angle. It means the block slide along the intersection of joint set 1 and joint set 3.

6.4 *The major key block projection view as result of key block theory programs*

Figure 40 shows the major removable block drawn by the key block program. The direction of each plane is defined by dip angle and dip direction angle. The coordinate of a given point on each plane is also entered in order to fix the location. The volume of the major block is 1.13 million cubic meters.

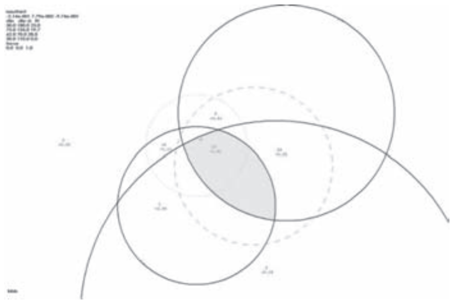

Figure 39. Finding sliding modes and factor of safety by whole stereographic projection.

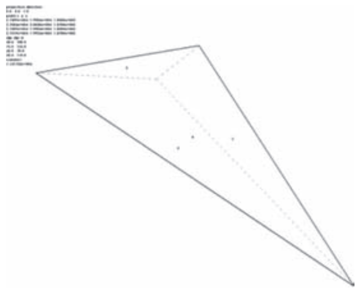

Figure 40. Three dimensional drawing of the major key block with projection direction (0.0, 0.0, 1.0).

Figure 41. Three dimensional DDA computation mesh of the major key block under gravity load.

Figure 42. Sliding process of the major key block under gravity load computed by 3-d DDA.

Figure 43. Sliding of the major key block under gravity load computed by 3-d DDA.

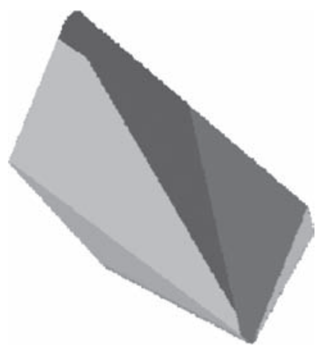

Figure 44. Three dimensional DDA computation of the major key block under gravity load and the previous tension forces of the cables.

6.5 *Three dimensional DDA computation of the major block stability*

Figures 41, 42, 43 and 44 are 3D-DDA computation. The load is gravity, no cable tension forces are applied. The friction angles are same as those in Figures 35 and 36. The block slides along the intersection line of plane 1 and plane 3 since the factor of safety is 0.67.

7 CONCLUSION

Applications of key block theory, 2-D DDA, 3-D joint cutting method and 3D DDA are presented in this paper. The key block theory is useful for the stability analysis of underground structure built in jointed hard rocks. Estimation of the removable blocks of a underground power house and surge chamber system were analyzed by the key block theory and 3D joint cutting method. Since DDA can reach limit equilibrium with large displacements, discontinuous contacts, precise friction law, multi-step computation and stabilized time-step dynamic computation, it is capable of study the damage and failure mechanisms of underground structure built in jointed rock. Two real applications, analysis of transportation tunnel and slopes, are represented. The stability analysis of a slope is also performed by a simple version of 3D DDA now available for modeling.

REFERENCE

Shi G.H. 1988. Discontinuous Deformation Analysis: A New Numerical Model for the Statics and Dynamics of Block Systems. PhD Thesis. University of California, Berkeley.

Shi G.H. 1993. Block system modeling by discontinuous deformation analysis. *Computational Mechanics Publications, Southampton*, UK and Boston, USA.

Shi G.H. 1999. Applications of discontinuous deformation analysis (DDA) and manifold method. *The Third International Conference on Analysis of Discontinuous Deformation, ICADD-3*, 3–15. Vail, Colorado.

Shi G.H. 2002. Single and multiple block limit equilibrium of key block method and discontinuous deformation analysis. Stability of Rock Structures, *ICADD-5*, 3–46. Beer Sheva, Israel.

Shi G.H. & Goodman, R.E. 1985. Two dimensional discontinuous deformation analysis. *Int. J. Numer. Anal. Methods Geomech.*,9: 541–556.

Shi G.H. & Goodman R.E. 1989. The key blocks of unrolled joint traces in developed maps of tunnel walls, *Int. J. Numer. Anal. Methods Geomech.,*13: 131–158.

Shi G.H., Goodman R.E. & Tinucci J.P. 1985. Application of block theory to simulated joint trace maps, *Proc. Int. Symp. on Fundamentals of rock joints*, 367–383, Bjorkliden (Sweden).

Advances in Discontinuous Numerical Methods and Applications in Geomechanics and Geoengineering – Zhao et al. (eds)
© 2012 Taylor & Francis Group, London, ISBN 978-0-415-68404-0

Recent developments and future trends in distinct element methods—UDEC/3DEC and PFC codes

José V. Lemos
LNEC—Laboratório Nacional de Engenharia Civil, Lisbon, Portugal

ABSTRACT: The Distinct Element Method was proposed by Cundall in 1971 as a numerical technique to study rock mechanics problems, based on the representation of a rock mass as a system of blocks or particles. In recent years, the concepts underlying such 'discontinuum' approaches were adopted innumerous other fields, and a multitude of formulations and codes were developed by many researchers. In this paper, the characteristic features of the codes UDEC/3DEC and PFC, ultimately descending from Cundall's original ideas, are analyzed with reference to various recent applications, within the global context of discrete element modeling. Modeling needs and trends of development in this field are finally discussed.

1 INTRODUCTION

The designation 'Discrete Element Method' (DEM) applies today to a wide class of numerical methods aimed at the simulation of the physical behavior of systems of particles, grains or blocks. The multiplicity of techniques, formulations, terminology and codes which can be included in this class is mainly a consequence of the historical development of these methods, in marked contrast with the finite element method (FEM). The latter's derivation from continuum mechanics allowed it to be consistently formulated as a numerical approximation of well-established differential equations. The existing continuum theories provided, in addition, a set of closed form solutions for validation of the numerical results, and for benchmarking the various codes. DEM followed a very different path, from the outset attempting to address problems that the continuum codes could not handle adequately, and for which no accepted theory existed. The representation of the interactions of the blocks or particles was designed mostly in an empirical manner, without reference to theoretical concepts, and the solutions of the various problems encountered in the development of the codes were reached in a pragmatic way, in order to solve specific applications. As a result, we have today an array of different DE methods, still in many ways marked by their origins and field of application.

Rock mechanics was one the fields of early DE model development, the major motivation being the discontinuous nature of fractured rock masses. For example, rock slope stability depended essentially on the frictional interaction between the blocks, not continuum deformation analysis, either elastic or plastic. Blocks could be assumed rigid given the low stresses involved, but failure mechanisms involved large movements and changes in block contact locations which invalidated the small displacement assumptions common in early numerical models. Conceptual models beyond continuum mechanics existed, e.g., the "clastic mechanics" proposal of Trollope (1968), but the analytical solution procedures limited their practical application. Cundall (1971) devised a general numerical solution technique capable of materializing the block assemblage concept, based on the time integration of the equations of motion of each block. The modeling of mechanical contacts between the blocks, which could now be assumed perfectly rigid, and the methods to detect them, completed the novel features of the designated 'Distinct element method'. Large displacement analysis became manageable, with the system connectivity automatically updated during a simulation,

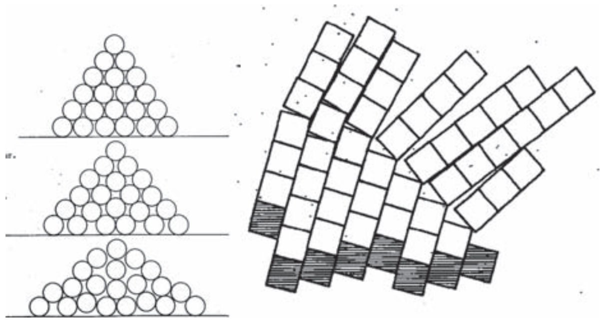

Figure 1. Two examples from Cundall's 1971 paper on the distinct element method: pile of disks and toppling failure mode of rock slope.

as some contacts break and new ones are formed as a consequence of the evolving geometry (Figure 1).

Discrete element concepts and methods have expanded considerably in recent years to a multitude of fields in science and engineering, where many related numerical techniques were developed for specific purposes. Discontinuous Deformation Analysis (DDA), Manifold Method (NMM), Discrete-Finite Elements (DFEM), Non-Smooth Contact Dynamics (NCSD), Molecular Dynamics (MD) and others methods, to be found in the proceedings of this conference orin the technical literature, all share the common concept of a "discontinuum". Underneath the differences in terminology, and the variety of numerical formulations, there are many common approaches, for example, to the representation of the mechanical contact between particles, or to the internal discretization of blocks to obtain complex deformation patterns. More instructive than comparing different methods or computer packages globally is to inspect specific components, examining the physical and constitutive assumptions employed and the way they are implemented numerically. This type of study will contribute to the necessary consolidation of concepts in the DE community, and assist the sharing of knowledge gained in different research areas. It is also important to accompany the new developments achieved by those researchers that continue to work under the FEM umbrella, such as contact-impact formulations, joint elements and strong embedded discontinuities, lattice models, XFEM, particle finite elements, and many others techniques that relate to the analysis of discontinuous systems.

This paper focuses on the line of DE model development following Cundall's approach, which led to the UDEC, 3DEC and PFC codes (Itasca 2007, 2008a, b, 2011). While the 'distinct element method' may be regarded formally as a sub-set of the 'discrete element' class, the two designations are used as synonyms by many authors, and this practice will be followed in this paper. Selected recent applications in various fields are discussed, with an emphasis on geomechanics modeling. Trends of future development and outstanding issues are finally addressed, both in terms of the physical and engineering problems that need to be solved, and of the computational aspects and code user requirements.

2 A REVIEW OF APPLICATIONS

2.1 *Fracture of geo-materials*

Rock mechanics is perhaps the field where a larger variety of DE models has been applied (e.g., Jing & Stephansson 2007). While the early efforts were intended to address engineering problems at the field scale, the potential of DE models to simulate the rock behavior at the scale of the lab test was soon recognized. The main motivation of the 2D circular particle code BALL presented by Cundall & Strack (1979) was to address the micro-mechanics of soils and other granular materials. However, by applying cohesive bonds between the particles, and letting them break in tension or shear, the same numerical formulation became the choice tool to study rock fracture, in the form of the bonded-particle models (BPM) (Potyondy & Cundall 2004). The random nature of the assemblies simulates the natural arrangement of grains in the rock matrix. Based on elementary constitutive laws governing the interaction between the rigid particles, complex forms of behavior develop, to be checked against experiments. In this active research field, developments on outstanding issues, such as the triaxial test behavior, are under way to improve the performance of bonded particle models (e.g., Cho et al., 2007, Potyondy 2010).

The fracture behavior of other geo-materials, such as concrete, may also be approached by these models, with different particles representing the aggregate and the cement paste (Azevedo & Lemos 2005). These authors introduced a general contact formulation for transmission of forces and moments between particles based on multiple contact points, as an alternative to the standard parallel bond model in PFC, which allows the progressive extension of the bond fracture between the two particles.

Analysis of the fundamental processes taking place during lab tests of rock joints have also been addressed. For example, Figure 2 (left) shows a very detailed particle model employed by Asadi & Rasouli (2011) to study the fracture patterns during shearing of a synthetic profile joint.

Polygonal block models, while computationally more costly, are perhaps capable of a closer representation of the rock matrix structure. They are more demanding, mainly because the contact calculations between polygons involve many more operations than those in circular particle codes. Various authors have nevertheless obtained very interesting results of fracture analysis with UDEC models. Damjanac et al. (2007) studied the micro-mechanical behavior of lithophysal tuff specimens with both particle (PFC) and block (UDEC) models (Figure 2).

Lan et al. (2010) represented the microstructure of brittle rock by means of a deformable polygonal grain-like assembly, to study the effect of heterogeneous grain deformability. Kazerani & Zhao (2010) used both Voronoi and Delaunay block assemblies in order to match experimental results of triaxial and Brazilian tests of rock specimens (Figure 3). Expanding the model size from lab test to field scale, while still difficult, is becoming feasible. Alzo'ubi et al. (2011) have studied the buckling failure of rock slopes with inclined layers with a UDEC model.

Most numerical fracture studies of rock lab tests to date only attempted to replicate the quasi-static response. The interest in dynamic fracture, however, has grown significantly (e.g., Zhao et al., 2011). Contact constitutive models capable of addressing dynamic rock fracture were implemented by Kazerani (2011), and tested in UDEC models.

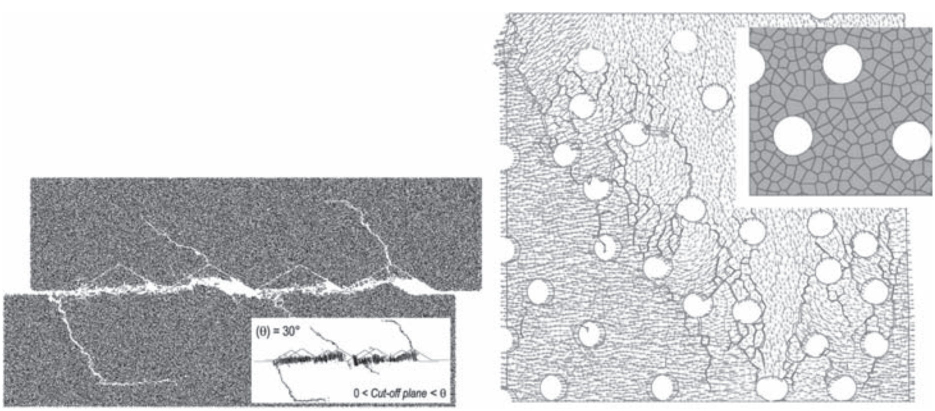

Figure 2. (left) Particle model of shear test of synthetic rock fracture profile (Asadi & Rasouli 2011); (right) UDEC model of uniaxial compression test on lithophysal tuff specimen (Damjanac et al., 2007).

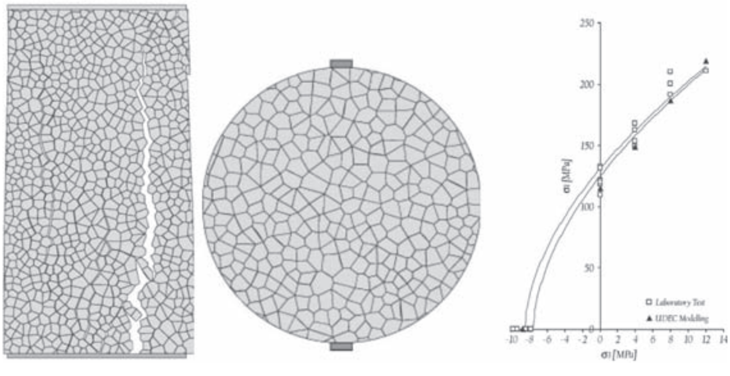

Figure 3. Rock specimens based on Voronoi polygons for simulation of uniaxial compression and Brazilian tensile tests and comparisons with experimental results (Kazerani & Zhao 2010).

2.2 *The synthetic rock mass (SRM) concept*

When going from the lab test to the field scale, the influence of rock macroscopic discontinuities comes into play. The rock joint structure may be represented in particle models by means of the Synthetic Rock Mass concept (SRM). A discrete fracture network (DFN) is overlaid on a particle assembly, thus partitioning it into a system of grains or blocks formed by bonded circular particles (Figure 4) (Pierce et al., 2007). Different properties are assigned to the bonds of the contacts between particles belonging to the same block, representing the intact rock material, and to the contacts between adjacent blocks, representing the joint behavior. The key to this approach lies in Cundall's Smooth Joint Model (SJM), applied to the inter-block contacts. Even if the interface is not an exact straight line, the SJM logic forces these contacts to adopt a common normal, leading to a smooth sliding governed by a prescribed friction angle. Otherwise, the very irregular nature of the contact surfaces would lead to unrealistic friction and dilation values.

Mas Ivars et al. (2008) have created a SRM with PFC3D to study scale effects in jointed rock masses. The anisotropic response and the trends in tensile and compressive strength variation were investigated by performing a series of numerical tests on samples of various sizes (Figure 5). Starting with a model of a $80 \times 40 \times 40$ m region, and then cutting it into smaller specimens, allowed a series of UCS tests, providing the trends in strength variation with sample size.

The run times for large 3D systems are still significant. Cundall (2011) proposed a faster alternative to PFC, the "lattice model", in which the finite-sized particles are replaced by point masses, and the contacts between particles are replaced by breakable springs. Assuming small displacements, it achieves high computational efficiency because the interaction geometry (location and apparent stiffness of springs) can be pre-computed, eliminating contact detection as an overhead. A lattice SRM model was applied by Cundall & Damjanac (2009) to the analysis of slopes with discontinuous joint sets, to study the fracture of the intact rock bridges (Figure 6).

2.3 *Concrete dam foundations*

The conceptual model of a rock mass as a blocky system has been employed for many years in the design of concrete dam foundations. A numerical DE model of an arch dam foundation may be viewed as an extension of classical block stability analysis. Instead of a single rock wedge, a block system is represented, and therefore, not just one, but multiple failure modes may be checked in a single run. Furthermore, block deformability can be considered, taking into account the dam-rock interaction, which could be relevant in valleys with marked heterogeneity. A key aspect in dam foundation problems is the effect of water pressures, which must be applied in the discontinuities (see section on coupled models below).

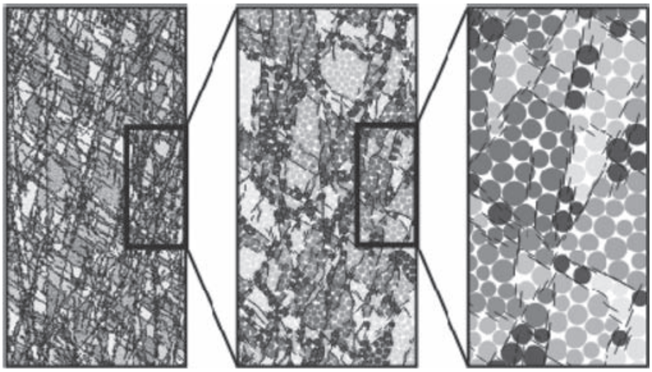

Figure 4. Synthetic rock mass (SRM) model (Pierce et al., 2007).

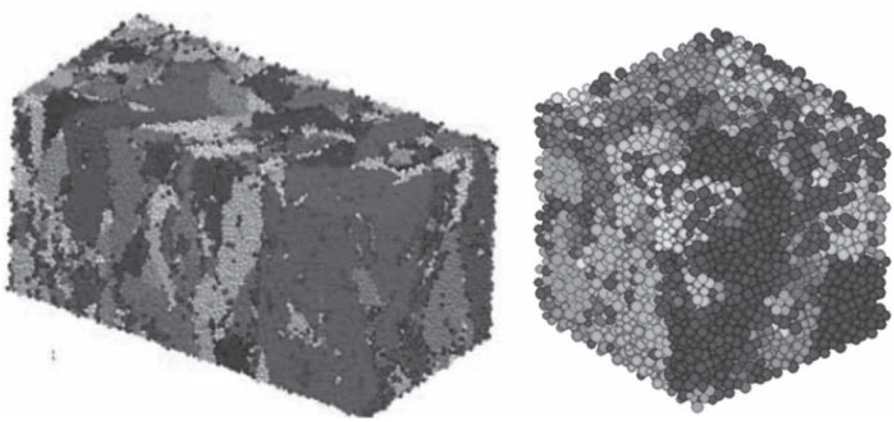

Figure 5. Three-dimensional SRM models: (left) view of the $80 \times 40 \times 40$ m model; (right) detail view of DFN inserted on PFC brick (Mas Ivars et al., 2008).

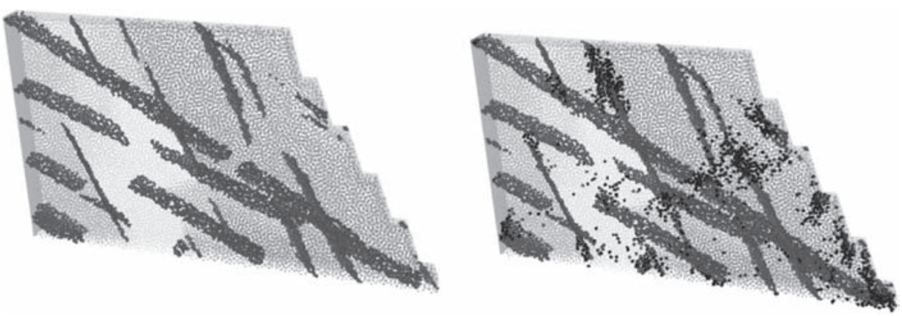

Figure 6. Cross-sectional slice through the upper part of a 1000-m slope modeled by SRM: (left) joint traces within the slice; (right) micro crack development (Cundall & Damjanac 2009).

In the study of arch dams, the correct representation of the deformability and stresses in the concrete shell is important. For this purpose, 3DEC allows meshes of 20-node brick finite elements in the concrete structure, while the rock mass blocks are still discretized with tetrahedra. This combination was used in the model of the 110 m high BaixoSabor dam (Figure 7) (Lemos & Antunes 2011). The model geometry was first established, including the surface

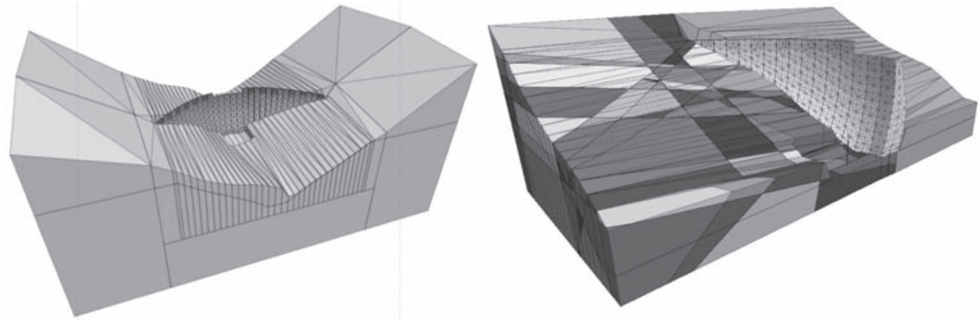

Figure 7. 3DEC model of BaixoSabor dam: (left) global model geometry before discontinuities are inserted; (right) detail of half of the block model with rock discontinuities (Lemos & Antunes 2011).

topography (left figure). The concrete-rock interface and the contraction joints between the cantilevers are also model discontinuities with nonlinear behavior. The major rock mass discontinuities were placed at their known locations, and then a few joints of each of the 3 main sets were selected. Safety factors for foundation failure modes were evaluated by progressive reduction of the joint strength properties, leading to the development of mechanisms as the one depicted in Figure 8.

2.4 *Underground excavations in rock*

A well-known early application of discontinuum models to underground works was the Gjovik cavern analysis by Barton et al. (1994), performed with a 2D UDEC model, in which the behavior of the discontinuities was represented by the Barton-Bandis joint model. The Tindaya cavern design was analyzed with 3DEC, involving a detailed representation of the rock mass discontinuities (Senís & Varona 2008). Figure 9 displays the unstable rock volumes in the roof and shaft sidewalls; an analysis with rock bolt support elements was subsequently performed.

Mining is a field where DE models have played an important role, as many problems involve conditions close to failure, whether in open pit or underground mining. The large displacement capabilities of these codes allow the simulations to proceed into the range of extensive material damage and breakage, for example, in cave mining problems (e.g., Sainsbury et al., 2011).

2.5 *Coupled problems*

The study of fluid flow in rock masses was one of the early motivations for coupled DE formulations. For example, in dam foundation studies, water pressures along the joints play a key role in stability. In gravity dam studies, mostly done in 2D, coupled hydro-mechanical analyses pose no computational difficulties. The blocks are typically assumed impervious, with all fluid flow taking place along the discontinuities. The example of Albigna dam, performed by Gimenes & Fernandez (2006) with UDEC, allowed an interesting comparison with dam monitoring results. A fracture flow model for 3DEC was developed by Damjanac (1996).

Nuclear waste isolation studies and petroleum engineering are two of the fields that drive the research on modeling of coupled processes in rock, and considerable recent literature exists on these subjects. For example, solute transport in networks of rock fractures was approached with UDEC models by Zhao et al. (2011), highlighting the importance of the stress effects on these processes. Hydraulic fracturing with a Synthetic Rock Mass model was addressed by Damjanac et al. (2010). In this particle model, fluid flow analysis was performed, allowing the fluid effects on propagation of fractures to be assessed.

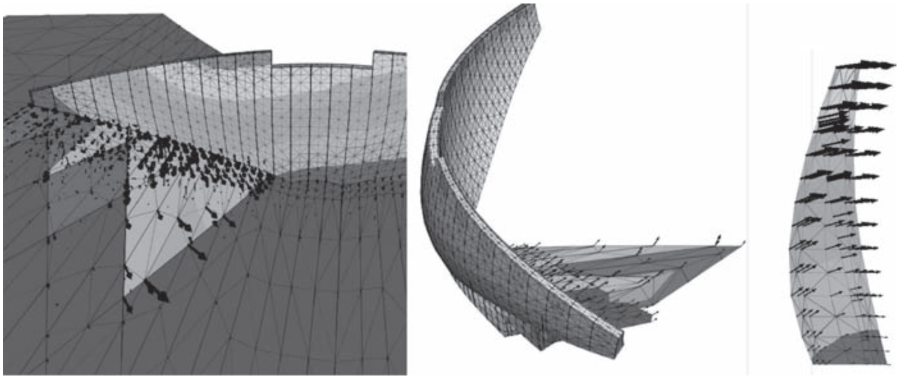

Figure 8. Nodal displacement vectors and contours denoting failure mechanism of arch dam foundation model obtained after progressive reduction of rock joint friction (Lemos & Antunes 2011).

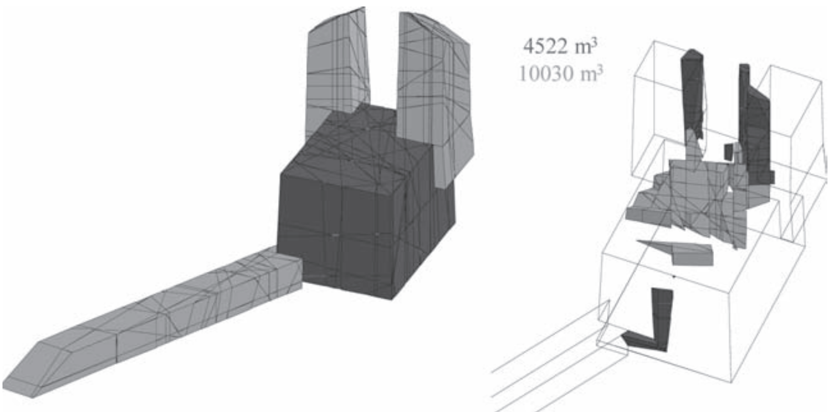

Figure 9. 3DEC model of Tindaya mountain project: (left) Excavation shapes; (right) Volumes of unstable rock in the unsupported case (Senís & Varona 2008).

2.6 *Masonry structures*

Stone masonry structures are one of the applications in which the assumptions of DE models are more closely reproduced. In fact, these structures are often made of regularly shaped blocks, and their exact geometry can be introduced in the numerical representation. In the case of dry joints, simple frictional models are fairly accurate. For competent stone materials, the assumption of block rigidity is also adequate. Therefore, DE models are now extensively used in this field, in particular for the seismic analysis of monuments and structures that are considered a valuable part of the architectural heritage. Figure 10 shows a 3DEC model of a section of the Parthenon Pronaos, in Athens (Psycharis et al., 2003). The rocking behavior of the drum columns is complex, and requires the consideration of large displacements and rotations. Arched structures and traditional constructions have also been studied (Figure 10).

2.7 *Rock fill and ballast models*

There are many systems that may be addressed by DE models, such as rock fill dams, railway ballast, or handling of bulk materials (e.g., Shimizu & Cundall 2001). Aikawa (2011) presents a three-dimensional dynamic numerical model for studies of a ballasted railway track using 3DEC (Figure 11). A discontinuous model of the ballasted track was created, comprising an

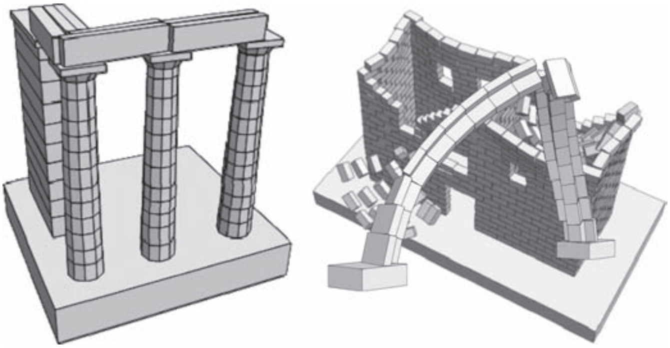

Figure 10. Rigid block models for seismic analysis of stone masonry. (left) Parthenon Pronaos (Psycharis et al., 2003); (center) free-standing arch (Lemos 2007); (right) traditional house (Alexandris et al., 2004).

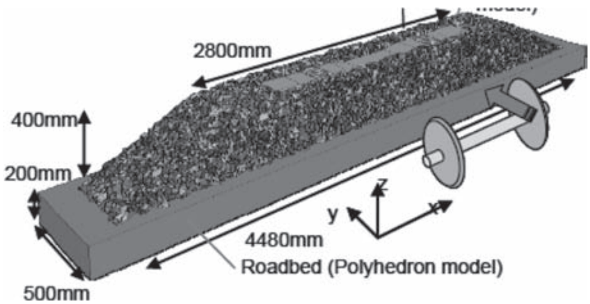

Figure 11. 3DEC model of ballasted railway track (Aikawa 2011).

assemblage of ballast polyhedrons, rail pads, sleepers, and a roadbed. The dynamic responses of track structure members in response to dynamic traffic loading of the train passing were simulated.

3 CURRENT ISSUES, MODELING NEEDS AND FUTURE TRENDS

3.1 *Modeling methodologies*

There are many available options for representing a given physical system by means of a numerical model, ranging from simplified continuous medium idealizations to very detailed DE simulations of its micro-structure. All of these have their role in science and engineering and the purpose of the analysis is a major factor in the choice of the most appropriate and effective. In engineering practice, models are often tools to answer a given question, regarding, for example, the suitability of a design aspect. Only the features that impact on the particular behavior under scrutiny need to be included in the model, so many details are better omitted. Starfield & Cundall (1988) addressed these and other methodological questions, namely how data limitations constrain the building of a model. The potential of the model as a numerical laboratory, to gain knowledge on the problem at hand, was also stressed.

The evolution of engineering modeling methodologies will progressively shape the manner in which DE codes are employed. The need for reliable tools capable of providing answers in a cost-effective manner will drive the design of general-purpose codes and their user interfaces. The importance of user interfaces is likely to grow, assuming a higher weight in development costs, as they tend to become a decisive factor in code selection.

3.2 *Interaction of multiple DE components*

As a consequence of the applications of flexible and adaptive modeling approaches, there is a tendency to employ various types of representations, even within the same project. Thus, it is becoming more important the transparent interchange of data between different models and codes. In the future, engineers will demand easier ways to build DE systems capable of mixing different types of elemental components, e.g., from spherical particles to macro-particles and polyhedral blocks, and interfacing them with FE meshes, always ensuring consistent physical interaction assumptions.

3.3 *Model building*

The tendency towards larger and more complex models implies that the tasks of model building take a larger percentage of the engineer's time. Improved procedures to create models are essential. This involves physical representation issues, as well as numerical aspects. For example, in rock mechanics, improved ways to describe and generate DFNs (discrete fracture networks), which better represent the natural rock mass state, are needed. In addition, efficient numerical procedures must be devised to materialize these DFNs in a particular DE code, offering the user simple and controllable means of model generation and verification.

The generation of large random particle assemblies in 3D is still a time consuming task. For large assemblies, setting initial stress states and driving strains according to prescribed paths have to be adequately thought. Furthermore, the procedures used to pack and load the particles may affect the mechanical response of the system, as discussed by Potyondy & Cundall (2004). In particular, for system geometries characterized by random parameters, it is essential to have automated ways to create many different samples with reduced user effort.

3.4 *Sound representation of physics*

The most distinctive feature of DE models is the contact formulation that governs the mechanical interaction between blocks or grains. The physical assumptions implied in the numerical implementation need to have solid foundations, and to be properly documented so that the user is aware of them, and may interpret the results accordingly. For example, whether the normal stiffness concept or a non-interpenetration assumption are employed, the numerical limitations and tolerances built into the contact detection and update procedures have to be consistent, robust and transparent to the user.

This requirement applies obviously to all the code essential components, from the use of FE meshes in deformable blocks, to fracturing and block splitting criteria. Continued validation of each specific feature against experimental data is mandatory to build confidence in the codes and their predictive capabilities.

3.5 *Coupled processes*

The importance of representing coupled physics processes will necessarily grow as more comprehensive treatment of phenomena is envisaged. Thermal-hydro-mechanical coupled models are currently used in various fields, with chemical parameters starting to be inserted into the common framework. With many interdependent variables, experimental validation becomes lengthy and more difficult, and a sound judgment is even more important in the assessment of numerical results.

3.6 *Access to data structures*

Many DE codes have been developed in research environments and are used mostly by their developers or other people within a relatively restricted environment. As these codes become available to wider audiences, the potential for erroneous use also increases. Large open-source projects have many merits, but also their own management difficulties. Commercial software invokes higher reliability, but drastically restricts the user autonomy, without the option to inspect the source or to modify it.

Granting the user access to the internal data structure, without the need to know the source details, delivers a much better degree of autonomy to the user, and also the ability to test and verify completely the code performance, and the manual's accuracy. The FISH language, developed by Cundall and implemented in UDEC/3DEC and PFC, is extremely useful in all modeling stages, namely in parameterized model generation, execution control or treatment of numerical or graphical output. For any code with a wide community of users, it is important to provide means to use the codes consistently, accessing all internal data structures without dependence on coding details or version changes.

3.7 *User-programmed constitutive models*

One of the critical factors in the choice of codes is the wealth of constitutive models offered. In DE codes, joint or contact constitutive models generally govern the system response. Giving the user the ability to program its own material models has greatly enhanced the software range of application. In particular, it extends the range of commercial codes in innovative research projects, to which they may bring all of their facilities for model generation and graphical user interfaces that special purpose codes often lack. User-defined constitutive models in UDEC/3DEC were initially written in the internal FISH language, but currently C++ is preferred, providing a standard programming framework. This also permits libraries of tested models to be built and made available to the user community.

Allowing the user to implement new constitutive assumptions without requiring knowledge of the internal code structure or changes in the source is an essential advantage for research-oriented projects. It also helps to clarify the relation between the assumptions about physical behavior and the strictly numerical issues.

3.8 *User interfaces*

As models become more elaborate, and codes offer a wider diversity of options, the design of user interfaces assumes a major role. Engineers demand robust and validated software packages capable of exploiting the available resources in an effective manner. It is particularly important that the codes are versatile, adaptable to the various levels of use, from the quick solution of fairly standard problems to the more elaborate types of analysis arising in research projects (Russell 2011).

Different users have their own preferences and requirements for the way they interact with the code. A novice user may prefer a well-designed menu interface, which simplifies the learning process and permits elementary problems to be set up without effort. An experienced user prefers more advanced procedures, possibly based on scripts or intelligible command files, which permit reuse of previous problem data, or the expedite creation of many related models. Of course, these procedures require learning time, and are only productive if frequent use of the code is intended. Ideally, a code interface should be flexible enough to allow both of these approaches. In particular, it is useful to be able to record interactive model building and execution, automatically creating command scripts that may be edited and reutilized.

For any type of user, high quality graphics are essential. The question of model verification, involving the checking of assigned properties, boundary or load conditions, and all critical input data items, is immensely aided by a good graphical interface.

3.9 *Analysis of results*

Analysis and interpretation of the results of a numerical simulation becomes increasingly difficult and time-consuming when advanced material behavior models are employed.

Often, the output of many parametric studies needs to be compared and synthesized. Internal programming languages, such as FISH, with access to the complete data structure of the problem, provide an excellent tool to treat the output of many runs, and create suggestive graphical representations.

Code output has evolved from large amounts of raw numbers to realistic graphical results. A further step is imperative to make the analyst's time more effective, by lending the codes better facilities to produce higher level indicators of performance, suited to the user needs.

Soft-computing techniques are now increasingly applied to assist in building knowledge from the results of numerical simulations. For example, DeGagné et al. (2011) used neural networks to develop behavior prediction tools for tunnels in squeezing ground, based on an extensive series of FLAC analysis.

3.10 *Computational aspects*

Run times remain the critical limit to analysis feasibility, as users continue to increase the size and complexity of their representations to take advantage of every advance in processor speed. There are clear trends to apply 3D models routinely to more problems, and to resort more frequently to dynamic, transient and coupled physics problems. Faster analyses are thus indispensable. Parallel processing techniques appear to be critical to achieve such goal. The availability of multiple core processors at reduced costs has already produced significant performance improvements, with multithreading techniques sometimes not involving substantial code redesign. However, various issues need to be addressed, for example, memory access management, as bandwidth limitations seriously affect performance (e.g., Williams et al., 2010, Russell 2011).

It should be noted that, in many research projects, large series of runs need to be undertaken. The time constraints depend not only on the run time of each analysis, but also on effective methods to treat and interpret output, as understanding of these results is indispensable to plan the runs ahead.

4 CONCLUSIONS

Over the years, advances in computer power haveal ways been matched by the increase in both size and complexity of numerical models. The pursuit of faster analyses, whether by means of parallel processing techniques or improved algorithms, remains a challenge for code developers. Nevertheless, it must be recognized that fairly intricate three-dimensional DE models are now routinely applied in engineering practice with very reasonable computational costs.

In DE modeling, finer representations or extended domain problems weigh substantially on the computational effort. Cundall (2001) argued that the future trend for numerical modeling in soil and rock may consist of the replacement of continuum methods by particle methods, as assemblies of discrete particles capture the complicated material behavior with simple assumptions and few parameters at the micro level. The research of the fundamental behavior of materials seems indeed to steer us from meso-scale to micro-scale, or even nano-scale analysis. In parallel with more elaborate models, engineering practice will continue to apply simplified continuous or coarse-grained block models, as long as these solve the problems at hand in a satisfactory and cost-effective manner. The articulation of a variety of models, tailored to different user needs, will certainly become easier to achieve and more prevalent.

The development of constitutive laws that better simulate the experimentally observed behavior and the focus on multi-physics coupled processes will continue to expand. However, as follows the discussion in the previous section, perhaps the most significant change in the future will be the way in which we use the codes. Advances in graphical user interfaces will improve substantially our ability to build large and complex representations, to automate the execution of extended series of parametric studies, and to extract from the output more elaborate and meaningful indicators of physical behavior or design performance, in order to advance our knowledge of the world and our engineering capabilities.

REFERENCES

Aikawa, A. 2011. DEM modeling techniques for dynamic analyses of ballasted railway track. In Sainsbury, Hart, Detournay & Nelson (eds), Continuum and Distinct Element Numerical Modeling in Geomechanics 2011, Paper 10–01.

Alexandris, A., Protopapa, E. & Psycharis, I. 2004. Collapse mechanisms of masonry buildings derived by the distinct element method. In 13th World Conf. Earthquake Eng., Vancouver, Paper no. 548.

Alzo'ubi, A.K., Martin, C.D. & Mughieda, O.G. 2011. Numerical modeling of buckling rock movement. In Sainsbury, Hart, Detournay & Nelson (eds), Continuum and Distinct Element Numerical Modeling in Geomechanics 2011, Paper 04–04.

Asadi, M.S. & Rasouli, V. 2011. PFC2D simulation of directionality in rough fractures shear strength.In Sainsbury, Hart, Detournay & Nelson (eds), Continuum and Distinct Element Numerical Modeling in Geomechanics 2011, Paper: 07–04.

Azevedo, N.M. & Lemos, J.V. 2005. A generalized rigid particle contact model for fracture analysis. Int. J. Numer. Analyt. Meth. Geomech. 29: 269–285.

Barton, N., By, T.L., Chryssanthakis, P., Tunbridge, L., Kristiansen, J., Loset, F., Bhasin, R.K., Westerdahl, H. & Vik, G. 1994. Predicted and measured performance of the 62 m span Norwegian olympic ice hockey cavern at Gjovik. Int. J. Rock Mech. Min. Sci. 31(6): 617–641.

Cho, N., Martin, C.D. & Sego, D.C. 2007. A clumped particle model for rock. Int. J. Rock Mech. Min. Sci., 44: 997–1010.

Cundall, P.A. 1971. A computer model for simulating progressive large scale movements in blocky rock systems, In Proc. Symp. Rock Fracture (ISRM), Nancy, vol. 1, paper II–8.

Cundall, P.A. 1987. Distinct element models of rock and soil structure. In E.T. Brown (ed.) Analytical and Computational Methods in Engineering Rock Mechanics, George Allen & Unwin, 129–163.

Cundall, P.A. 2001. A discontinuous future for numerical modelling in geomechanics? Proc. Inst. Civil Engineers, Geotechnical Engineering, 149(1): 41–47.

Cundall, P.A. 2011. Lattice method for modeling brittle, jointed rock. In Sainsbury, Hart, Detournay & Nelson (eds), Continuum and Distinct Element Numerical Modeling in Geomechanics—2011, Paper 01–02.

Cundall, P.A. & Damjanac, B. 2009. A Comprehensive 3D Model for Rock Slopes Based on Micromechanics, In Slope Stability 2009, Universidad de Los Andes, Santiago, Chile.

Cundall, P.A. & Strack, O.D.L. 1979. A discrete numerical model for granular assemblies. Geotechnique, 29(1): 47–65.

Damjanac, B. 1996. A three-dimensional numerical model of water flow in a fractured rock mass. PhD Thesis, University of Minnesota, Minneapolis, USA.

Damjanac, B., Board, M., Lin, M., Kicker, D. & Leem, J. 2007. Mechanical degradation of emplacement drifts at Yucca Mountain—A modeling case study. Part II: Lithophysal rock. Int. J. Rock Mech. Min. Sci., 44: 368–399.

Damjanac, B., Gil, I., Pierce, M., Sanchez, M., Van As, A. & McLennan, J. 2010. A New Approach to Hydraulic Fracturing Modeling in Naturally Fractured Reservoirs. 44th US Rock Mechanics Symposium, Paper 10–400, ARMA.

DeGagné, D.O., Corkum, A.G. & Lorig, L. 2011. Estimation of tunnel squeezing in anisotropic stress fields using a FLAC-based neural network. In Sainsbury, Hart, Detournay & Nelson (eds), Continuum and Distinct Element Numerical Modeling in Geomechanics—2011, Paper: 03–06.

Detournay, C. & Dzik, E. 2006. Nodal Mixed Discretization for Tetrahedral Elements. In Hart & Varona (eds) Numerical Modeling in Geomechanics 2006, Paper 07–02.

Farinha, M.L.B., Lemos, J.V. & Maranha das Neves, E. 2011. Numerical modelling of borehole water-inflow tests in the foundation of the Alqueva arch dam. Can. Geotech. J., 48(1): 72–88.

Gimenes, E. & Fernandez, G. 2006. Hydromechanical analysis of flow behavior in concrete gravity dam foundations. Can. Geotech. J., 43: 244–259.

Hart, R.D., Cundall, P.A. & Lemos, J.V. 1988. Formulation of a three-dimensional distinct element model—Part II: Mechanical calculations for motion and interaction of a system composed of many polyhedral blocks. Int. J. Rock Mech. Min. Sci., 25: 117–125.

Itasca 2007. 3DEC (3-Dimensional Distinct Element Code), Version 4.1, Minneapolis, Minnesota.

Itasca 2008a. PFC2D (Particle Flow Code in 2 Dimensions), Version 4.0, Minneapolis, Minnesota.

Itasca 2008b. PFC3D (Particle Flow Code in 3 Dimensions), Version 4.0, Minneapolis, Minnesota.
Itasca 2011. UDEC (Universal Distinct Element Code), Version 5.0, Minneapolis, Minnesota.
Jing, L. & Stephansson, O. 2007. Fundamentals of Discrete Element Methods for Rock Engineering—Theory and Application, Elsevier.
Kazerani, T. 2011. Micromechanical study of rock fracture and fragmentation under dynamic loads using discrete element method. PhD thesis, Ecole Polytechnique Fédérale de Lausanne (EPFL), Lausanne.
Kazerani, T. & J. Zhao 2010. Micromechanical parameters in bonded particle method for modeling of brittle material failure. Int. J Num. Analyt. Meth. in Geomech., DOI: 10.1002/nag.884.
Lan, H., Martin, C.D. & Hu, B. 2010. Effect of heterogeneity of brittle rock on micromechanical extensile behavior during compression loading. J. Geophysical Research, 115, B01202.
Lemos, J.V. 2007. Discrete element modeling of masonry structures. International Journal of Architectural Heritage, 1(2): 190–213.
Lemos, J.V. 2008. Block modelling of rock masses—Concepts and application to dam foundations. European Journal of Environmental and Civil Engineering, 12(7–8): 915–949.
Lemos, J.V. 2011. Discontinuum models for dam foundation failure analysis. In QihuQian & Yingxin Zhou (eds.) Harmonizing rock engineering and the environment, 12th ISRM Congress, Beijing, CRC Press, 91–98.
Lemos, J.V. & Antunes, N.S. 2011. Modelling of arch dam foundation failure scenari—Case studies of BaixoSabor and Alto Ceira dams. Dam Engineering, XXI(4): 299–312.
Mas Ivars, D., Pierce, M., DeGagné, D. & Darcel, C. 2008. Anisotropy and Scale Dependency in Jointed Rock-Mass Strength—A Synthetic Rock Mass Study. In Hart, Detournay & Cundall (eds) Continuum and Distinct Element Numerical Modeling in Geo-Engineering 2008, Paper 06–01.
Pierce, M., Cundall, P., Potyondy, D. & Mas Ivars, D. 2007. A Synthetic Rock Mass Model for Jointed Rock. In E. Eberhardt et al. (eds) Rock Mechanics: Meeting Society's Challenges and Demands (1st Canada-U.S. Rock Mech. Symp., Vancouver), vol. 1, London: Taylor & Francis, 341–349.
Potyondy, D. 2010. A Grain-Based Model for Rock: Approaching the True Microstructure. In Li et al. (eds) Proc. Rock Mechanics in the Nordic Countries 2010, Oslo, 225–234.
Potyondy, D.O. & Cundall, P.A. 2004. A bonded-particle model for rock. Int. J. Rock Mech. Min. Sci., 41:1329–64.
Psycharis, I.N., Lemos, J.V., Papastamatiou, D.Y., Zambas, C. & Papantonopoulos, C. 2003. Numerical study of the seismic behaviour of a part of the Parthenon Pronaos. Earthquake Eng Struct. Dyn., 32: 2063–2084.
Russell, D. 2011. The next generation of Itasca software. http://www.flacdemsymposium.com (consulted 31 October 2011).
Sainsbury, B.L., Sainsbury, D.P. & Pierce, M.E. 2011. A historical review of the development of numerical cave propagation simulations. In Sainsbury, Hart, Detournay & Nelson (eds), Continuum and Distinct Element Numerical Modeling in Geomechanics 2011, Paper 02–02.
Senís, M. & Varona, P. 2008. 3DEC numerical modeling of the Tindaya Mountain Project. In Hart, Detournay & Cundall (eds) Continuum and Distinct Element Numerical Modeling in Geo-Engineering 2008, Paper 07–07.
Shimizu, Y. & Cundall, P.A. 2001. Three-Dimensional DEM Simulations of Bulk Handling by Screw Conveyors, J. Engng. Mech., 127(9): 864–872.
Starfield, A.M. & Cundall, P.A. 1988. Towards a methodology for rock mechanics modelling. Int. J. Rock Mech. Min. Sci., 25(3): 93–106.
Trollope, D.H. 1968. The mechanics of discontinua or clastic mechanics in rock problems. In K.G. Stagg & O.C. Zienkiewicz (eds) Rock Mechanics in Engineering Practice, John Wiley, 275–320.
Williams, J.R., Holmes, D. & Tilke, P. 2010. Multi-core strategies for particle methods. In A. Munjiza (ed.) Discrete element methods—Simulations of discontinua: theory and applications, Queen Mary, University of London, 11–17.
Zhao, J., Zhou, Y.X. & Xia, K.W. 2011. Advances in rock dynamics modelling, testing and engineering. In QihuQian & YingxinZouh (eds.) Harmonizing rock engineering and the environment, 12th ISRM Congress, Beijing, CRC Press, 147–154.
Zhao, Z., Jing, L., Neretnieks, I. & Moreno, L. 2011. Numerical modeling of stress effects on solute transport in fractured rocks. Computers & Geotechnics, 38: 113–126.

Advances in Discontinuous Numerical Methods and Applications in Geomechanics and Geoengineering – Zhao et al. (eds)
 ISBN 978-0-415-68404-0

Application of DDA and NMM to practical problems in recent new insight

Y. Ohnishi & T. Koyama
Kyoto University, Kyoto, Japan

T. Sasaki & I. Hagiwara
Rock Engineering Lab., Suncoh Consultants Co. Ltd., Tokyo, Japan

S. Miki
Kisojiban Consultants Co. Ltd., Tokyo, Japan

T. Shimauchi
Meiji Consultants Co. Ltd., Saitama, Japan

ABSTRACT: The authors introduced for the practical problems by using 2D-DDA, 2D-NMM, 2D-Coupled analysis of NMM and DDA and 3D-DDA in recent new insight. Categories of the analysis are distributed 2D-DDA dynamic rock fall problems and its sensitive analysis between the velocity ratio and the penalty, Earthquake response analysis of rock slopes, 2D-NMM, 2D-coupled analysis of DDA and NMM and 3D-DDA rock fall problem. Model of Bayon temple at Angkor Thom in Cambodia as the world heritages of UNESCO is analyzed. The authors evaluated the applicability of the methods and the reliability of the results by comparisons between different methods and site observations for the practical problems.

1 INTRODUCTION

1.1 *Japanese research group activity*

Japanese research group for working in the discontinuous analyses were introduced by Ohnishi et al. (2006, 2007). This paper introduces the discontinuous methods using DDA and NMM for the rock failure of slope stability triggered by earthquakes, heavy rain falls by typhoons as frequently occurred in Japan island during recent past few years. Especially, March 11th 2011, a massive scale earthquake of magnitude 9.0 occurred on the pacific coast along from Sanriku to Ibaraki coast. Also Tsunami occurred in a vast area for hundreds of kilometers from off-shore Iwate at coast of Ibaraki Prefectures. Over 19,000 people are died or unknown and lost over 330,000 houses around shore side. In addition the disaster caused serious trouble for Japanese people due to the failure of the Fukushima nuclear power plants.

1.2 *Recent new insight of Japanese group research work*

The authors introduce three main practical problems by using DDA and NMM such as the slope stability, the earthquake response analysis and the ancient masonry structures to maintain the world heritages in UNESCO activities. The ancient masonry structure in Bayon Temple of Angkor Tom in Cambodia is analyzed using DDA+NMM coupled analysis (Koyama, et al., 2011). Two rock fall problems are introduces as Jinro and Soun valley in Hokkaido and the parameter studies concerning in the time increment and the penalty